



# The Operating Room Global Journal (TORGJ)

<https://torgjournal.org/>

ISSN: 3105-3262



## Morphology And Morphometry of Right Ventricular False Tendons

Vincent Kipkorir<sup>1</sup>, Charity Kobuthi<sup>1,3\*</sup>, Talha Chaudhry<sup>1</sup>, Mohamed Onyango<sup>1</sup>, Stephanie Momanyi<sup>1</sup>, Musa Misiani<sup>1</sup>, Jeremiah Munguti<sup>1</sup>, Beda Olabu<sup>2</sup>

<sup>1</sup>Department of Human Anatomy and Physiology, University of Nairobi, Kenya.

<sup>2</sup>Department of Biomedical Sciences, Aga Khan University, Kenya.

<sup>3</sup>The Operating Room Global (TORG).

### ABSTRACT

#### \*Corresponding Author:

Charity Kobuthi

[kobuthicharity8@gmail.com](mailto:kobuthicharity8@gmail.com)

#### Declaration:

**Authors' Contribution:** VK: Study conception, data collection, analysis, and manuscript drafting; CK, TC, MO: Protocol development and manuscript editing; SM: Data analysis and manuscript editing; MM, JM, BO: Data management and manuscript editing. All authors approved the final manuscript.

**Conflict of Interest:** No conflict of interest.

**Funding:** No funding received.

**Background:** False tendons (FTs) are fibrous or fibromuscular structures, that traverse the cavity of the ventricles and have no attachment to valvular cusps. In contrast to the well documented Left ventricular false tendons, right ventricular false tendons (RFTs) remain poorly understood, with only a five-type classification system in use. RFTs are clinically significant and have been implicated in S3 gallops, ventricular arrhythmias and systolic murmurs. Moreover, their presence increases the possibility of catheter entanglement and incorrect diagnosis during cardiac procedures.

**Materials and Methods:** Sixty-eight hearts from formalin-fixed cadavers from the Department of Human Anatomy, University of Nairobi were used in this study. The hearts were incised, false tendons identified, classified and lengths measured from origin to insertion using a digital Vernier caliper, accurate to 0.01 cm. Data was analyzed using SPSS Version 25.0. Prevalence was reported with 95% Wilson confidence intervals; lengths were expressed as means and standard deviations. Group differences were assessed using Kruskal-Wallis and Mann-Whitney U tests ( $\alpha = 0.05$ ).

**Results:** RFTs were identified in 63.2% of examined hearts, with a mean of 1.4 types per heart (range: 1-4). Beyond the five conventionally defined types (Types 1-5), six novel types were observed. Across all 122 false tendons, Type 1 (septum to anterior papillary muscle) was the most prevalent overall (18.9%). Within Type 11 (tricuspid leaflets to septum, moderator band, and posterior ventricular free wall), those extending from the septal leaflet to the septum were most common (33.6%). Mean false tendon length was  $14.6 \pm 7.1$  mm (range: 1-34 mm). Type 3 (anterior tricuspid leaflet to RV free wall) was the longest ( $25.5 \pm 6.4$  mm), while Type 9 (septum to moderator band) was the shortest (8.0 mm).

**Conclusion:** RFTs are prevalent anatomical variations that exhibit more morphological diversity than previously documented. These results offer a thorough anatomical reference that is essential for preventing complications during right-sided cardiac interventions, understanding abnormal valvular mechanics and distinguishing RFTs from pathologies during imaging.

**Keywords:** Right Ventricle; False Tendons Classification; Morphometry; Cardiac Anatomy; Tricuspid Valve

#### Article History:

Received: 30-05-2026

Accepted: 09-06-2026

Available Online: 10-06-2026

#### QR access this Article



## INTRODUCTION

False tendons (FTs), first described by Turner in 1893 and thereafter by Keith and Flack in 1906 are defined as single or multiple, thin, fibrous or fibromuscular structures that traverse the cavity of the ventricles and have no attachment to valvular cusps [1,2]. Variations exist in the structure of right ventricular false tendons (RFTs) with regard to their origin, connection with the right ventricular free wall and to papillary muscles. Five types have been described by Loukas et al. [3], regarding the RFTs based on their location and attachments. In Type I, RFTs are located between the ventricular septum and the anterior papillary muscle; in Type II, they are located between the ventricular septum and the posterior papillary muscle; in Type III, between the anterior leaflet of the tricuspid valve and the right ventricular free wall; in Type IV, between the posterior papillary muscle and the ventricular free wall; while in Type V between the anterior papillary muscle and ventricular free wall.

Clinically, FTs have been suggested as possible substrates in several heart pathologies including ventricular arrhythmias, gallops, and systolic murmurs [4]. They have also been reported to cause catheter entanglement during cardiac catheterization procedures [5]. Imaging procedures have also misinterpreted false tendons for flail valve chordae tendineae or mural thrombi [6-8]. With the growing use of echocardiography, cardiac MRI, and right-heart interventional procedures including transcatheter tricuspid valve interventions and electrophysiological mapping, accurate anatomical knowledge of RFTs has become increasingly relevant to modern clinical practice. Current anatomical classification systems for RFTs remain limited, and the lack of a comprehensive characterization creates challenges for both imaging interpretation and procedural planning.

Previous workers have majorly focused and extensively explored Left Ventricular False Tendons (LFTs) [1,2,6-13]; however, to the best of our knowledge, very few studies have explored RFTs [3,14,15]. This study therefore aimed to further explore and describe the anatomical features of the RFTs with regards to morphometry and morphology.

## MATERIALS AND METHODS

All available formalin-fixed hearts from the cadaveric repository of the Department of Human Anatomy, University of Nairobi were consecutively screened for inclusion in this study. Hearts with grafts, traumatic lesions, any observable signs of autolysis, or heart pathologies such as cardiomegaly were excluded. Demographic data (age, sex, ethnicity, and cause of death) were not available for the cadaveric specimens, as is common with previously dissected institutional repositories; this represents a recognized limitation of the study.

An inter-caval incision was made to open the right atrium, extending from the orifice of the superior vena cava to the orifice of the inferior vena cava. Additionally, another incision was made on the right border of the heart to expose the cavity of the right ventricle. False tendons were identified and classified by two experienced anatomists. Intra-observer repeatability was assessed by having each observer remeasure a random subset of 20 RFTs after a 2-week interval. Inter-observer reliability was assessed for all measurements. False tendon lengths were measured twice from origin to insertion using a digital Vernier caliper accurate to 0.01 cm, and the mean of the two measurements was recorded.

Classification was performed according to the following locations: Type I: between ventricular septum and anterior papillary muscle; Type II: between ventricular septum and posterior papillary muscle; Type III: between the anterior leaflet of the tricuspid valve and right ventricular free wall; Type IV: between posterior papillary muscle and ventricular free wall; Type V: between anterior papillary muscle and ventricular free wall. Novel types (Types 6-11) were defined de novo based on structural features that could not be accommodated within the existing five-type classification; the rationale for each new category is detailed in the Results.

Representative photos were taken using a 12-megapixel Nokia camera (Model: RM-596). Prevalence of each RFT type was expressed as a percentage of the total number of false tendons identified ( $n = 122$ ), with 95% confidence intervals (CIs) calculated using the Wilson score method, which is robust for small proportions. False tendon lengths were entered into SPSS software (Version 25.0, Chicago, Illinois) and expressed as means and standard deviations (SD); 95% CIs for mean length were computed using the t-distribution for types with  $n \geq 2$ .

Types represented by a single observation ( $n = 1$ ) are reported descriptively only. Global between-group differences in false tendon length across all types were assessed using the Kruskal-Wallis H test, which is non-parametric and appropriate given the small and unequal group sizes; post-hoc pairwise comparisons were not performed owing to insufficient sample sizes within individual type groups. Additionally, Mann-Whitney U tests were used to compare: (i) prevalence and length between classic (Types 1-5) and novel types (Types 6-11); and (ii) length between septum-attached and non-septum-attached tendons. A Kruskal-Wallis test was also applied across Type 11 subtypes. Statistical significance was set at  $\alpha = 0.05$ . Intra-class correlation coefficients (ICC) were calculated for both intra-observer (ICC = 0.94, 95% CI: 0.88-0.97) and inter-observer (ICC = 0.91, 95% CI: 0.84-0.95) repeatability, indicating excellent agreement.

## RESULTS

Of the 68 hearts examined, right ventricular false tendons (RFTs) were observed in 43 cases (63.2%). The mean number of types of false tendons per heart ranged from 1-4, with a mean of 1.4 types per heart. The total number of false tendons studied was 122. Among the conventionally defined types (Types 1-5), Type 1 (ventricular septum to anterior papillary muscle) was the most prevalent classic type ( $n = 23$ ; 18.9%, 95% CI 12.9-26.7%). However, when all 11 types are considered, Type 11 (tricuspid leaflets to septum, moderator band, and posterior ventricular free wall) had the highest cumulative prevalence ( $n = 66$ ; 54.1%, 95% CI 45.3-62.7%). Beyond the conventionally defined types (Types 1-5), six novel types were observed with attachments as follows: Type 6: interconnecting papillary muscles; Type 7: septum to posterior ventricular free wall; Type 8: septum to septal papillary muscle; Type 9: septum to moderator band; Type 10: septal papillary muscle to moderator band; Type 11: tricuspid leaflets to septum, moderator band and posterior ventricular free wall.

Type 1 was the most prevalent classic type ( $n = 23$ ; 18.9%, 95% CI 12.9-26.7%), while Types 7, 9 and 10 showed the least prevalence ( $n = 1$  each; 0.8%, 95% CI 0.1-4.5%). Among interpapillary tendons (Type 6;  $n = 7$ ; 5.7%, 95% CI 2.8-11.4%), those linking anterior and posterior papillary muscles showed the highest subtype prevalence (4.1%), while connections involving the septal papillary muscle were least prevalent (0.8% each). Within Type 11 ( $n = 66$ ; 54.1%, 95% CI 45.3-62.7%), those extending from the septal leaflet to the septum were most prevalent (33.6%), while those linking the septal leaflet to the posterior ventricular free wall were least prevalent (0.8%). Full prevalence values with 95% confidence intervals for all types are provided in Tables 1 and 2.

The mean length of all false tendons was  $14.6 \pm 7.1$  mm (range 1-34 mm). Type 3 (anterior tricuspid leaflet to RV free wall;  $n = 2$ ) was the longest at  $25.5 \pm 6.4$  mm, while Type 9 (septum to moderator band;  $n = 1$ ) was the shortest at 8.0 mm. Among the types with sufficient sample sizes, 95% confidence intervals for mean length were: Type 1, 14.3-17.9 mm; Type 4, 3.9-12.7 mm; Type 5, 5.6-15.2 mm; Type 6, 14.1-18.3 mm; and Type 11, 13.5-15.9 mm. For Types 2, 3, and 8, CIs were wide and clinically uninformative owing to very small sample sizes ( $n = 2-3$ ), and these types should be interpreted descriptively.

A Kruskal-Wallis H test across all types with  $n \geq 2$  demonstrated statistically significant global heterogeneity in false tendon length ( $H = 19.847$ ,  $df = 7$ ,  $p = 0.006$ ). Post-hoc pairwise comparisons between individual types were not performed owing to insufficient sample sizes within most groups; larger studies are needed to confirm specific between-type differences. Comparison of septum-attached tendons (Types 1, 2, 7, 8, 9, and septal subtypes of Type 11;  $n = 96$ ; mean 15.6 mm) versus non-septum-attached tendons (Types 3, 4, 5, 6, 10;  $n = 26$ ; mean 12.5 mm) revealed a statistically significant difference in length (Mann-Whitney  $U = 1565.0$ ,  $p = 0.048$ ). No significant difference in length was found between classic and novel types (Mann-Whitney  $U = 1620.0$ ,  $p = 0.611$ ), nor between Type 11 and all other types combined.

(Mann-Whitney  $U = 1895.0$ ,  $p = 0.811$ ). Within Type 11 subtypes, Kruskal-Wallis analysis across the four subtypes with  $n \geq 3$  (anterior leaflet→septum, posterior leaflet→septum, septal leaflet→septum, septal leaflet→moderator band) did not demonstrate statistically significant length differences ( $H = 5.069$ ,  $p = 0.167$ ).

Among tendons interconnecting papillary muscles (Type 6), those spanning from septal to anterior papillary muscles were the longest (26.0 mm;  $n = 1$ ), while those connecting anterior and posterior papillary muscles were the shortest (9.6 mm; mean). Within Type 11, tendons from the septal leaflet to the septum were the longest ( $17.2 \pm 7.0$  mm), while those linking the anterior leaflet to the septum were the shortest ( $11.3 \pm 8.5$  mm).

## DISCUSSION

The present study found right ventricular false tendons in 63.2% of the examined hearts. This high prevalence supports early historical assertions by Turner in 1893 and Keith and Flack in 1906 that these structures are a constant feature in mammalian hearts. Our findings are consistent with those of Mundra et al. [14] and Loukas et al. [3], who found right ventricular false tendons in majority of the adult hearts in their studies. The frequency observed in our current study suggests that RFTs are a typical anatomical variation of the right ventricular morphology rather than an incidental anomaly, further supported by Sanchez et al. [11], who demonstrated that false tendons are normal findings present from fetal development through adulthood.

According to our morphological analysis, Type 1 (septum to anterior papillary muscle) accounted for the highest proportion of conventionally defined RFTs (18.9%). This is consistent with Loukas et al. who reported septum to papillary muscle connections as the most prevalent type. However, our findings are in contrast with those of Kosiński et al. [15] who report Type V; connections between the walls of the ventricle around its apex and Mundra and Lala [14] who report Type 1 papillary muscle to free wall connections as their most prevalent type. These discrepancies might be explained by the different method of dissection, demographics and classification systems.

In addition to the five types initially reported by Loukas et al. [3], we observed more morphological diversity. Specifically, we identified six more types (Types 6-11), with Type 11 having a cumulative prevalence of 54.1%. Although conventional literature tends to confine RFTs to either simple interpapillary or septomarginal connections, our findings of common attachments between the tricuspid leaflets and the septum (33.6%) suggest a more integrated association between RFTs and the valvular apparatus than has been documented before. Regarding valvular mechanics, these connections could potentially limit the movement of the tricuspid leaflets during systole and may provide an anatomical basis for future investigation of valve dynamics or functional tricuspid regurgitation; however, confirmation requires clinical and imaging studies. This provides an anatomical basis to understand how these chords may influence the dynamics of the tricuspid valve or lead to misdiagnosis.

The current study found a mean false tendon length of  $14.6 \pm 7.1$  mm (range 1-34 mm). Type 3 (anterior tricuspid leaflet to RV free wall;  $n = 2$ ) was the longest at  $25.5 \pm 6.4$  mm, while Type 9 (septum to moderator band;  $n = 1$ ) was the shortest at 8.0 mm. Kruskal-Wallis analysis demonstrated statistically significant global heterogeneity in false tendon length across types ( $H = 19.847$ ,  $p = 0.006$ ). Post-hoc pairwise comparisons between individual types were not performed given inadequate sample sizes within most groups, underscoring the need for larger prospective studies. Notably, septum-attached tendons were significantly longer than non-septum-attached tendons (mean 15.6 vs 12.5 mm;  $p = 0.048$ ), which may be anatomically relevant given the greater intracavitary span required to bridge septal to contralateral structures. No significant length difference was found between classic and novel types ( $p = 0.611$ ), suggesting that the novel morphological variants described here are broadly comparable in size to previously documented types.

Mundra and Lala [14] found papillary muscle-to-free wall connections to be the longest and septomarginal trabeculae connections the shortest, while Kosiński et al. [15] qualitatively identified interpapillary muscle connections as the longest

and intrapapillary muscle segment connections as the shortest. The present study's shortest type is anatomically comparable to the shortest reported by Mundra and Lala [14], both involving septal or trabecular connections. The longest type varied across comparable studies, likely reflecting differences in population characteristics and dissection methods. These measurements are clinically important because imaging techniques have mistakenly identified false tendons for mural thrombi or flail valve chordae tendineae [6]. The morphometric variability observed here, combined with the significant elongated nature of several types, raises the possibility that these structures may appear as mobile, linear echoes on echocardiography, warranting greater caution in distinguishing them from pathological structures.

Literature indicates that some RFTs contain myocardial fibers and conducting tissue identical to the bundle of His [3]. Suwa et al. [12] and Perry et al. [13] have reported an association between false tendons and premature ventricular contractions (PVCs), although a direct causal link has not been definitively established. The anatomical locations of specific RFTs identified in the present study, particularly those involving connections between the septum, papillary muscles, and moderator band, are consistent with reported arrhythmogenic substrates given the distribution of the right bundle branch and Purkinje fibres in these regions. It must be noted that no histological examination was performed in the present study; accordingly, claims regarding arrhythmogenic potential of the newly identified types remain speculative and require future histological confirmation.

Notably, a causal relation between FTs and both an S3 gallop and a systolic murmur has been noted in the literature [4]. Moreover, the identification of Type 11 RFTs in the present study, which bridge the tricuspid leaflets to the septum and free wall, provides a possible anatomical explanation for the catheter entanglement reported by Winrow et al. [5] during right-sided cardiac procedures. The morphological and morphometric findings from the present study provide clinicians with a comprehensive anatomical reference to predict possible substrates for arrhythmias, abnormal valve dynamics, and procedural complications in the right ventricle.

#### **Limitations and recommendations for further studies.**

There are several limitations to this study. The age and sex of the cadavers were not accounted for, as this study relied on human hearts from a previously established repository for which demographic records were unavailable. Given that cardiac morphology may vary with age, sex, and ethnicity, the absence of this information reduces the interpretability and generalizability of findings; future studies should prospectively record full demographic data. Additionally, the classification system proposed here represents observational categories derived by two anatomists from a single population; while consensus was reached on all novel types, independent validation by multiple observers and replication in diverse populations will be necessary before the classification can be adopted widely. Tissue shrinkage could have occurred due to formalin fixation, which could potentially affect the accuracy of length measurements. The morphometric analysis was limited to linear measurements and as such, future studies should incorporate cross-sectional measurements such as thickness to give a more detailed morphometric profile. Histological examination and analysis were not conducted in the current study; further studies are needed to support or refute the presence of conducting tissue within the newly described types to define their arrhythmogenic capability. Lastly, the absence of a standardized classification and dissection methodology across RFT research limits the possibility of direct cross-study comparisons; subsequent research should adopt a standardized methodology to allow for more meaningful synthesis and comparison of results.

## **CONCLUSION**

Right ventricular false tendons (RFTs) are common anatomical variations that exhibit significant morphological diversity. Because these structures frequently resemble mural thrombi or flail chordae during imaging, their morphometric variability and elongated nature may trigger diagnostic confusion. Additionally, their close proximity to the conducting system could potentially provide a substrate for clinical observations such as ventricular arrhythmias, S3 gallops, and systolic murmurs. Our findings offer a comprehensive anatomical reference that may help raise intervention safety and improve diagnostic precision.

**Declaration of interest:** We have no conflicts of interest

**Ethical statement:** This study was conducted in accordance with the Human Anatomy Act (CAP 249, 1976) and the Human Tissues Act (CAP 252, 1968) of the Laws of Kenya. Ethical approval was obtained from the Department of Human Anatomy and Physiology, University of Nairobi (approving authority: Departmental Ethics and Research Committee, Approval reference number: HAMP BAUEC/2018/266; Date 28th March, 2018). This manuscript has been carried out in accordance with the Code of Ethics of the World Medical Association (Declaration of Helsinki) and is in line with the Recommendations for the Conduct, Reporting, Editing and Publication of Scholarly Work in Medical Journals.

**Author contributions CrediT :**

VK: project protocol development, data collection and analysis and manuscript writing.

CK: project protocol development and manuscript editing.

TC: project protocol development and manuscript editing.

MO: project protocol development and manuscript editing.

SM: data analysis and manuscript editing.

MM: data management and manuscript editing.

JM: data management and manuscript editing.

BO: data management and manuscript editing.

**Funding statement:** This research did not receive any specific grant from funding agencies in the public, commercial, or not-for-profit sectors.

**Acknowledgements:** No acknowledgements to declare.

## REFERENCES

- [1] L.M. Gerlis, H.M. Wright, N. Wilson, F. Erzençin, D.F. Dickinson, Left ventricular bands. A normal anatomical feature., *Heart* 52 (1984) 641-647. <https://doi.org/10.1136/hrt.52.6.641>.
- [2] M. Kervancıoğlu, D. Özbağ, P. Kervancıoğlu, E.S. Hatipoğlu, M. Kilinç, F. Yılmaz, M. Deniz, Echocardiographic and morphologic examination of left ventricular false tendons in human and animal hearts, *Clin. Anat.* 16 (2003) 389-395. <https://doi.org/10.1002/ca.10152>.
- [3] M. Loukas, C.T. Wartmann, R.S. Tubbs, N. Apaydin, R.G. Louis, B. Black, R. Jordan, Right ventricular false tendons, a cadaveric approach, *Surg. Radiol. Anat.* 30 (2008) 317-322. <https://doi.org/10.1007/s00276-008-0326-5>.
- [4] K.R. Sethuraman, R. Sriram, J. Balachandar, Left ventricular false tendons: echocardiographic incidence in India and clinical importance, *Int. J. Cardiol.* 6 (1984) 385-387. [https://doi.org/10.1016/0167-5273\(84\)90201-8](https://doi.org/10.1016/0167-5273(84)90201-8).
- [5] D. Winrow, C.F. Beckmann, J.M. Lacomis, C.G. Dedrick, Entanglement of a pigtail catheter by the chordae tendineae of the tricuspid valve during pulmonary angiography, *Cardiovasc. Intervent. Radiol.* 19 (1996) 275-277. <https://doi.org/10.1007/BF02577649>.
- [6] P.H. Luetmer, W.D. Edwards, J.B. Seward, A. Jamil Tajik, Incidence and distribution of left ventricular false tendons: An autopsy study of 483 normal human hearts, *J. Am. Coll. Cardiol.* 8 (1986) 179-183. [https://doi.org/10.1016/S0735-1097\(86\)80110-3](https://doi.org/10.1016/S0735-1097(86)80110-3).
- [7] A. Casta, W.J. Wolf, Left ventricular bands (false tendons): Echocardiographic and angiographic delineation in children, *Am. Heart J.* 111 (1986) 321-324. [https://doi.org/10.1016/0002-8703\(86\)90147-X](https://doi.org/10.1016/0002-8703(86)90147-X).
- [8] M. Sugiyama, T. Nishimura, M. Kondo, H. Umadome, Y. Shimono, Echocardiographic features of false tendons in the left ventricle, *Am. J. Cardiol.* 48 (1981) 177-183. [https://doi.org/10.1016/0002-9149\(81\)90588-9](https://doi.org/10.1016/0002-9149(81)90588-9).

- [9] A.K. Abdulla, A. Frustaci, J.E. Martinez, R.A. Florio, J. Somerville, E.G.J. Olsen, Echocardiography and Pathology of Left Ventricular "False Tendons," *Chest* 98 (1990) 129-132. <https://doi.org/10.1378/chest.98.1.129>.
- [10] M. Loukas, R.G. Louis, B. Black, D. Pham, M. Fudalej, M. Sharkees, False tendons: An endoscopic cadaveric approach, *Clin. Anat.* 20 (2007) 163-169. <https://doi.org/10.1002/ca.20347>.
- [11] F. Sánchez Ferrer, M.L. Sánchez Ferrer, M.D. Grima Murcia, M. Sánchez Ferrer, F. Sánchez Del Campo, Basic Study and Clinical Implications of Left Ventricular False Tendon. Is it Associated With Innocent Murmur in Children or Heart Disease?, *Rev. Esp. Cardiol. Engl. Ed.* 68 (2015) 700-705. <https://doi.org/10.1016/j.rec.2014.09.021>.
- [12] M. Suwa, Y. Hirota, K. Kaku, Y. Yoneda, A. Nakayama, K. Kawamura, K. Doi, Prevalence of the coexistence of left ventricular false tendons and premature ventricular complexes in apparently healthy subjects: A prospective study in the general population, *J. Am. Coll. Cardiol.* 12 (1988) 910-914. [https://doi.org/10.1016/0735-1097\(88\)90453-6](https://doi.org/10.1016/0735-1097(88)90453-6).
- [13] L.W. Perry, R.N. Ruckman, S.R. Shapiro, K.S. Kuehl, F.M. Galioto, L.P. Scott, Left ventricular false tendons in children: Prevalence as detected by 2-dimensional echocardiography and clinical significance, *Am. J. Cardiol.* 52 (1983) 1264-1266. [https://doi.org/10.1016/0002-9149\(83\)90584-2](https://doi.org/10.1016/0002-9149(83)90584-2).
- [14] P. Mundra, B.S. Lala, A Study of Human Right Ventricular False Tendons: Morphology and Its Clinical Significance, *Indian J. Appl. Res.* 6 (2016) 162-164.
- [15] A. Kosiński, M. Grzybiak, A. Dubaniewicz, K. Kędziora, W. Makarewicz, D. Kozłowski, False chordae tendineae in right ventricle of adult human hearts - morphological aspects, *Arch. Med. Sci.* 5 (2012) 834-840. <https://doi.org/10.5114/aoms.2012.31617>.

## TABLES AND FIGURES

**Table 1: Prevalence and length of right ventricular false tendon types 1-5**

Type	n (Prevalence %; 95% CI)	Length mm, Mean ± SD (95% CI)
1. Ventricular septum and anterior papillary muscle	23 (18.9; 95% CI 12.9-26.7)	16.1±4.2 (95% CI 14.3-17.9)
2. Ventricular septum and posterior papillary muscle	3 (2.5; 95% CI 0.8-7.0)	15.0±6.9 (95% CI n/a, n=3)
3. Anterior tricuspid leaflet and right ventricular free wall	2 (1.6; 95% CI 0.5-5.8)	25.5±6.4 (95% CI n/a, n=2)
4. Posterior papillary muscle and ventricular free wall	7 (5.7; 95% CI 2.8-11.4)	8.3±4.8 (95% CI 3.9-12.7)
5. Anterior papillary muscle and ventricular free wall	9 (7.4; 95% CI 3.9-13.4)	10.4±6.3 (95% CI 5.6-15.2)
Cumulative frequency & mean length	44 (36.1; 95% CI 28.1-44.9)	14.0±6.6† (95% CI 12.0-16.0)

**Table 2: Prevalence and length of right ventricular false tendon types 6-11**

Type	n (Prevalence %; 95% CI)	Length mm, Mean ± SD (95% CI)
6. Interconnecting papillary muscles	7 (5.7; 95% CI 2.8-11.4)	16.2±2.3 (95% CI 14.1-18.3)
7. Septum to posterior ventricular free wall	1 (0.8; 95% CI 0.1-4.5)	20.0 (n=1)

8. Septum to septal papillary muscle	2 (1.6; 95% CI 0.5-5.8)	11.0±9.9 (95% CI n/a, n=2)
9. Septum to moderator band	1 (0.8; 95% CI 0.1-4.5)	8.0 (n=1)
10. Septal papillary muscle to moderator band	1 (0.8; 95% CI 0.1-4.5)	9.0 (n=1)
11. Tricuspid leaflets to septum, moderator band and posterior ventricular free wall	66 (54.1; 95% CI 45.3-62.7)	14.7±4.9 (95% CI 13.5-15.9)
Cumulative frequency & mean length	78 (63.8; 95% CI 55.1-71.9)	14.6±5.1 (95% CI 13.5-15.8)

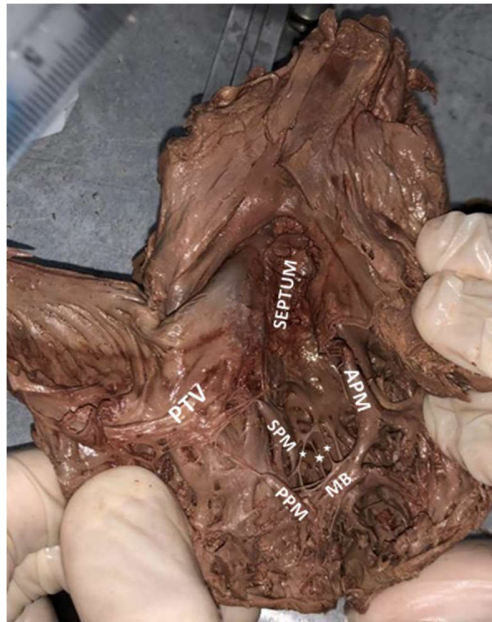
**Table 3: Prevalence and length of right ventricular false tendons associated with tricuspid leaflets**

Type	n (Prevalence %; 95% CI)	Length mm, Mean ± SD (95% CI)
Anterior leaflet to septum	10 (8.2; 95% CI 4.5-14.4)	11.3±8.5 (95% CI 5.2-17.4)
Posterior leaflet to septum	11 (9.0; 95% CI 5.1-15.4)	14.2±6.8 (95% CI 9.6-18.8)
Septal leaflet to septum	41 (33.6; 95% CI 25.8-42.4)	17.2±7.0 (95% CI 15.0-19.4)
Septal leaflet to moderator band	3 (2.5; 95% CI 0.8-7.0)	15.0±2.0 (95% CI 10.0-20.0)
Septal leaflet to posterior ventricular free wall	1 (0.8; 95% CI 0.1-4.5)	16.0 (n=1)
Cumulative frequency & mean length	66 (54.1; 95% CI 45.3-62.7)	15.7±7.4 (95% CI 13.9-17.5)

**Table 4: Prevalence and length of right ventricular false tendons interconnecting papillary muscles**

Type	n (Prevalence %; 95% CI)	Length (mm) Mean ± Std.
Anterior and posterior papillary muscle	5 (4.1; 95% CI 1.8-9.2)	9.6±7.0 (95% CI 1.0-18.2)
Posterior and septal papillary muscles	1 (0.8; 95% CI 0.1-4.5)	13.0 (n=1)
Septal and anterior papillary muscle	1 (0.8; 95% CI 0.1-4.5)	26.0 (n=1)
Cumulative frequency & mean length	7 (5.7; 95% CI 2.8-11.4)	16.2±2.3 (95% CI 14.1-18.3)

**Figure 1. Type 9 right ventricular false tendons (asterisks) extending from the interventricular septum to the moderator band (MB). APM: anterior papillary muscle;**



PPM: posterior papillary muscle; SPM: septal papillary muscle; PTV: posterior tricuspid valve leaflet.



Figure 2. Two co-existing right ventricular false tendon types. Asterisk: Type 11a false tendon extending from the septal tricuspid leaflet to the interventricular septum. Arrows: Type 10 false tendon extending from the septal papillary muscle (SPM) to the moderator band (MB). APM: anterior papillary muscle; PPM: posterior papillary muscle; STV: septal tricuspid valve leaflet

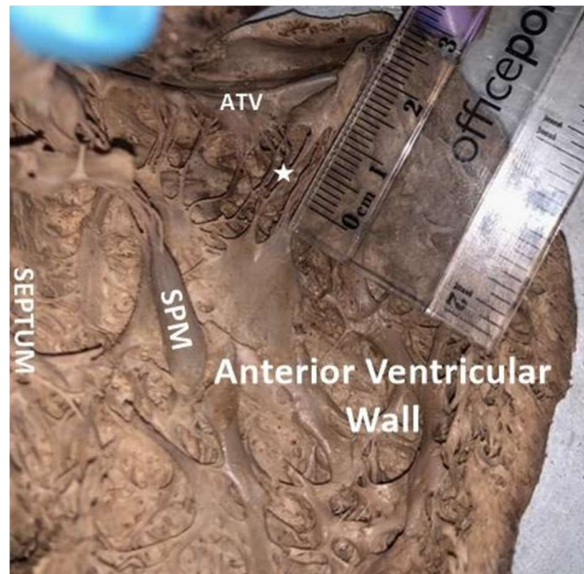


Figure 3. Type 3 right ventricular false tendon (asterisk) extending from the anterior tricuspid valve leaflet (ATV) to the anterior right ventricular free wall. SPM: septal papillary muscle.



Figure 4. Type 7 right ventricular false tendon (arrows) extending from the interventricular septum to the posterior ventricular wall (PVW). ATV: anterior tricuspid valve leaflet; PTV: posterior tricuspid valve leaflet; STV: septal tricuspid valve leaflet.



Figure 5. Type 9 right ventricular false tendon (arrow) extending from the moderator band (MB) to the interventricular septum. APM: anterior papillary muscle; PPM: posterior papillary muscle; ATV: anterior tricuspid valve leaflet; PTV: posterior tricuspid valve leaflet; STV: septal tricuspid valve leaflet.

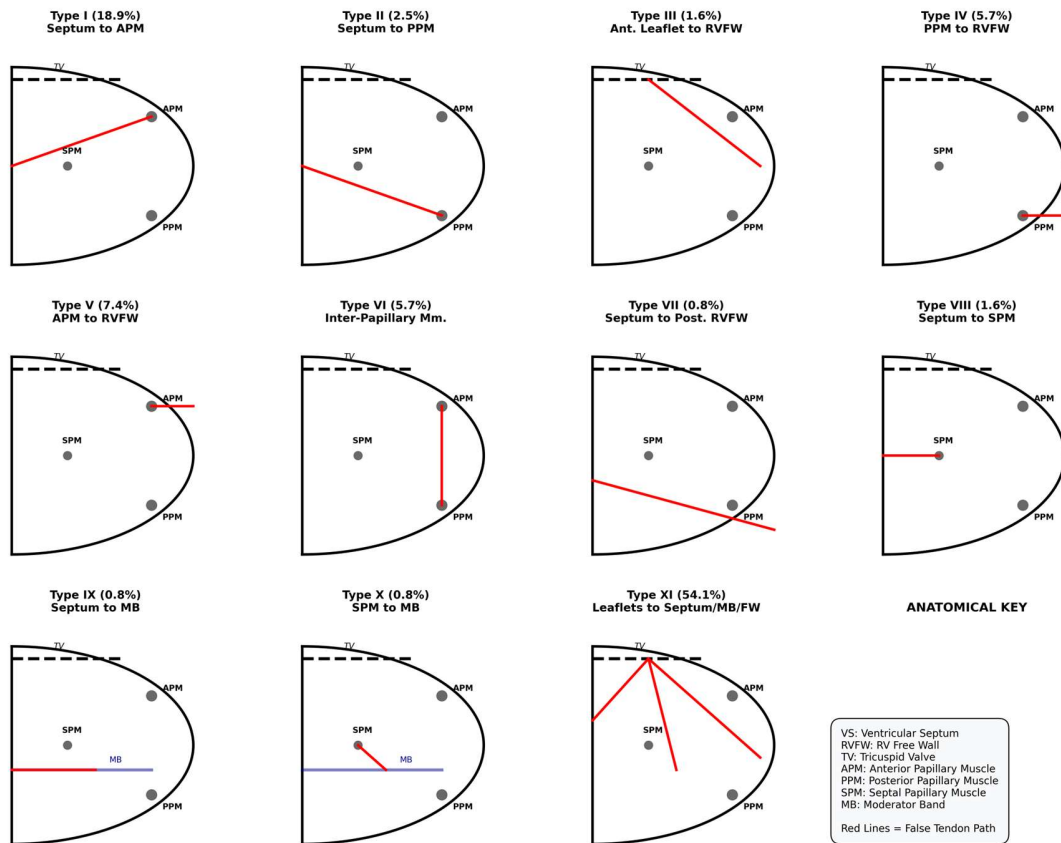


Figure 6: Schematic representation of the right ventricular false tendon (RFT) classification system. The diagram depicts the eleven morphological types (Types I-XI) based on their origins and insertions, with percentages indicating their relative frequencies. Types I-V correspond to the classic Loukas classification, while Types VI-XI represent the novel variants identified in this study. Red lines trace the course of each false tendon. Anatomical landmarks are provided in the key.

## CITE THIS ARTICLE:

- **APA (7th edition):** Kipkorir, V., Kobuthi, C., Chaudhry, T., Onyango, M., Momanyi, S., Misiani, M., Munguti, J., & Olabu, B. (2026, June 10). *Morphology and morphometry of right ventricular false tendons. The Operating Room Global Journal (TORGJ)*, 2(2). <https://doi.org/10.64573/torgj2605009>
- **Harvard:** Kipkorir, V., Kobuthi, C., Chaudhry, T., Onyango, M., Momanyi, S., Misiani, M., Munguti, J. and Olabu, B., 2026. *Morphology and morphometry of right ventricular false tendons. The Operating Room Global Journal (TORGJ)*, 2(2). Published 10 June. Available at: <https://doi.org/10.64573/torgj2605009>
- **Vancouver:** Kipkorir V, Kobuthi C, Chaudhry T, Onyango M, Momanyi S, Misiani M, Munguti J, Olabu B. Morphology and morphometry of right ventricular false tendons. *The Operating Room Global Journal (TORGJ)*. 2026 Jun 10;2(2). <https://doi.org/10.64573/torgj2605009>
- **MLA (9th edition):** Kipkorir, Vincent, et al. "Morphology and Morphometry of Right Ventricular False Tendons." *The Operating Room Global Journal (TORGJ)*, vol. 2, no. 2, 10 June 2026, <https://doi.org/10.64573/torgj2605009>
- **Chicago (Author-Date):** Kipkorir, Vincent, Charity Kobuthi, Talha Chaudhry, Mohamed Onyango, Stephanie Momanyi, Musa Misiani, Jeremiah Munguti, and Beda Olabu. 2026. "Morphology and Morphometry of Right Ventricular False Tendons." *The Operating Room Global Journal (TORGJ)* 2 (2), June 10. <https://doi.org/10.64573/torgj2605009>